Biochemical Pharmacology 78 (2009) 1205–1213

Contents lists available at ScienceDirect

Biochemical Pharmacology

journal homepage: www.elsevier.com/locate/biochempharm

Macrophage inhibitory cytokine-1 (MIC-1) and subsequent urokinase-type plasminogen activator mediate cell death responses by ribotoxic anisomycin in HCT-116 colon cancer cells

Hyun Yang [a], Hye Jin Choi [a], Seong Hwan Park [a], Jong Sik Kim [b], Yuseok Moon [a,*]

[a] Department of Microbiology and Immunology and Medical Research Institute, Pusan National University School of Medicine, Yangsan 626-813, Republic of Korea
[b] Department of Biological Science, Andong National University, Andong, Republic of Korea

ARTICLE INFO

Article history:
Received 4 April 2009
Accepted 11 June 2009

Keywords:
Macrophage inhibitory cytokine-1 (MIC-1)
Urokinase-type plasminogen activator
Anisomycin
Colon cancer

ABSTRACT

Ribosome-inactivating stresses possess a potent regulatory activity against tumor cell progression. In this study, we demonstrated that macrophage inhibitory cytokine-1 (MIC-1) and its associated signals determined the colon cancer cell response to the chemical ribotoxic stress. The ribotoxic stress agent anisomycin-induced MIC-1 gene expression which was involved in the ribotoxin-induced apoptotic pathway. MIC-1 was also a critical inducer of apoptosis-related gene products such as activated urokine-type plasminogen activator (PLAU) and PLAU receptor (uPAR). When MIC-1 or PLAU action was repressed in the tumor cells, the chemical ribotoxic stress triggered a survival-related MAP kinase such as ERK. Mechanistically, gene expression of apoptosis-mediator MIC-1 was enhanced by activating transcription factor 3 (ATF-3) via the p38 MAP kinase signaling pathway. Moreover, both promoter activity and mRNA stability of MIC-1 gene were up-regulated by ribotoxic anisomycin via the p38 MAP kinase signaling pathway. In conclusion, ribotoxic anisomycin-induced MIC-1 expression via p38–ATF3 pathway and subsequent apoptosis while suppressing survival ERK signal in the colon cancer cells. The results of this study provide mechanistic insight into tumor cell decision for death or survival pathways in response to ribosome-disrupting stresses from chemotherapeutics.

1. Introduction

Macrophage inhibitory cytokine-1 (MIC-1, also known as PTGF-ß, PLAB, GDF15, PDF, NAG-1, and PL74), is a transforming growth factor-ß superfamily cytokine that is involved in epithelial tumor pathogenesis [1–3]. In the normal epithelial cells, there is little or no detectable expression of MIC-1. However, with epithelial neoplastic transformation, the level of MIC-1 expression rises dramatically, and this is further increased in response to a variety of anti-tumorigenic stimuli, such as gamma irradiation, anti-inflammatory phytochemicals or non-steroidal anti-inflammatory drugs (NSAIDs) [4,5]. During the early stages of tumorigenesis, elevated MIC-1 may lead to tumor cell apoptosis, inhibition of blood vessel formation, and tumor cell cycle arrest, collectively referred to as the chemo-preventive activity. MIC-1 can be induced either in p53-depedent or – independent way and its inductive cellular signals also include other diverse growth-regulatory triggers [6–8].

Specific ribosome-directed xenobiotics have the capacity to damage 28S ribosomal RNA by interfering with its activity during gene translation. This can lead to what has been labeled as ribotoxic stress responses, which stimulate intra-cellular sentinel signaling pathways. This process results in the expression of genes important in cellular homeostasis as well as a variety of pathogenic processes [9,10]. Anisomycin, UV radiation, ricin and a variety of sesquiterpenoid trichothecene fungal metabolites have been reported to be effective triggers of the ribotoxic stress response in cells because these xenobiotics bind to the 28S ribosomal RNA peptidyltransferase site, block protein synthesis and can activate stress signals [11]. The bacterial compound anisomycin, secreted by *Streptomyces* spp., inhibits translation by binding to the 60S ribosomal subunits and blocking peptide bond formation, thereby preventing elongation and causing polysome stabilization [12]. Since the primary toxic action of most ribotoxic stress agents is generally recognized to be the functional inhibition of the global protein synthesis, highly dividing tissues such as lymphoid tissue and gastrointestinal epithelium are known to be the most susceptible targets of toxic insult [13–15]. Moreover, ribotoxic stress agents can cause cellular apoptosis or sensitize tumor cells to death factor-induced apoptosis [16,17]. Whereas normal intestinal epithelial cells undergo apoptotic cell death referred to as anoikis after detachment from the extracellular matrix, the malignant cells can survive anoikis-mediated death signals and migrate with metastatic potential [18]. A recent chemical biology

* Corresponding author. Tel.: +82 51 510 8094; fax: +82 55 382 8090.
E-mail address: moon@pnu.edu (Y. Moon).

0006-2952/$ – see front matter © 2009 Elsevier Inc. All rights reserved.
doi:10.1016/j.bcp.2009.06.012

study identified anisomycin as an anoikis sensitizer in malignant tumor cells [19]. Acquisition of resistance to apoptosis is a defining feature of tumor cells. Ribosome-inactivating chemotherapeutic drugs including anisomycin have been demonstrated to facilitate a death ligand-mediated apoptotic pathway in the malignant tumor cells [20,21].

In association with the ribotoxic stress response, various intracellular sentinel signaling pathways have been implicated. Anisomycin has been widely investigated as an extremely potent activator of kinase cascades in mammalian cells, especially the stress-activated mitogen-activated protein (MAP) kinase subtypes [22–24]. Depending on the cell types, toxicant-induced disruption of ribosomal homeostasis has been associated with the activation of stress signals such as c-Jun N-terminal kinase (JNK) and p38 MAPK (mitogen-activated protein kinase) and/or alterations in extracellular-signal-regulated kinase (ERK) 1/2 signaling [11,25]. In particular, p38 and JNK play key roles in apoptotic cell death by the ribosome-inactivating agents [15,26]. Unlike genotoxic or non-ribotoxic agent-induced cytotoxicity, the ribotoxic stress response requires intact active ribosomes. Disruption of the ribosomal integrity potentiates the sentinel signals such as MAP kinases in a few minutes followed by the induction of immediate gene subsets such as early growth response gene 1 (EGR-1) and activating transcription factor 3 (ATF-3) [27,28].

The serine protease urokinase-type plasminogen activator (PLAU) and its receptor (PAR) are involved in a variety of different physiological and pathological responses. uPAR, binding to the growth factor-like domain of PLAU, mediates transmembrane signals via the extracellular proteolysis, thus regulating tissue regeneration, angiogenesis, cancer growth and metastasis [29]. Recent studies show a close relationship of the PLAU system and tumor cell survival/apoptosis [30,31]. PLAU is responsible for modulation of the cell proliferation/apoptosis ratio through the dynamic control of cell–matrix interactions. Moreover, MIC-1 is known to up-regulate PLAU system in the gastric carcinoma, suggesting cooperative contribution to the regulation of cancer progression [32,33].

Associated with the ribotoxic stress responses, MIC-1 and subsequent associated signals were assessed for its involvement in colon epithelial cancer cell growth or survival. We investigated the effects of ribotoxic anisomycin on related signaling pathways for MIC-1 induction. Moreover, the potential roles of MIC-1 induction were addressed in terms of the cellular stress pathways leading to cell death or survival. The goal of this study was to provide mechanistic insight into the tumor cell responses to ribotoxic stresses associated with MIC-1 induction.

2. Materials and methods

2.1. Cell culture conditions and reagents

Human colon carcinoma HCT-116 and ilocecal HCT-8 cells were purchased from the American Type Culture Collection (Rockville, MD, USA) and maintained in RPMI 1640 medium (Invitrogen) supplemented with 10% (v/v) heat-inactivated fetal bovine serum (FBS, Sigma–Aldrich, St. Louis, MO, USA), 50 unit/ml penicillin (Sigma–Aldrich), and 50 μg/ml streptomycin (Sigma–Aldrich) in a 5% CO_2 humidified incubator at 37 °C. Cell number and viability were assessed by trypan blue (Sigma–Aldrich) dye exclusion using a hemacytometer. All of the chemicals were purchased from Sigma (Sigma–Aldrich).

2.2. Cell viability assay

Colorimetric analysis of cell growth was performed with Thiazolyl Blue Tetrazolium Bromide (MTT) assay. Cells (5×10^4/well) were cultured in 96-well plate for each time and the MTT (20 μl from 5 mg/ml stock solution) was added to the cells for 2 h. The supernatant was removed and the pellet was dissolved with 200 μl dimethyl sulfoxide (DMSO). The optical density was read at 560 nm with the background at 670 nm subtracted. The optical density was directly correlated with the quantity of cells.

2.3. Cell cycle analysis and apoptosis quantification by flow cytometry

Trypsinized cells (1×10^6) were prepared and re-suspended in 0.2 ml of PBS. Following the addition of 0.2 ml heat-inactivated fetal bovine serum, the cells were immediately fixed by slow dropwise addition of 1.2 ml ice-cold 70% (v/v) ethanol with gentle mixing, and then incubated at 4 °C overnight. The cells were washed and incubated with 1 ml propidium iodide (PI) DNA staining reagent (PBS containing 50 μg/ml PI, 50 μg/ml RNase A, 0.1 mM EDTA, and 0.1% (v/v) Triton X-100) on ice until analyzed. The cell cycle distribution for single cells was measured with a Becton Dickinson FACS Calibur (San Jose, CA, USA). Data from 10,000 cells were collected in the list mode. The 488 nm spectral line of an argon laser was used to excite the PI, and fluorescence was detected at 615–645 nm. The cell cycle of individual cells was studied using a doublet discrimination gating method that eliminates doublets and cell aggregates based on the DNA fluorescence. The gate was calibrated to include hypofluorescent cells. Cells in the DNA histogram with hypofluorescent DNA were designated as apoptotic. All other cells were distributed to give a normal cell cycle profile.

Cells to be examined for annexin V expression were washed twice with phosphate-buffered saline (PBS), 1×10^6 cells were re-suspended in 100 μl 1× binding buffer (10 mM HEPES/NaOH, pH 7.4, 140 mM NaCl, 2.5 mM $CaCl_2$), containing 4 μl FITC-annexin V (BD biosciences) stock and 2.5 μl 2 mg/ml propidium iodide (PI). After incubation for 15 min in the dark at room temperature, 400 μl 1× binding buffer was added to each tube and in a light-protected area, the specimens were quantified by flow cytometry, with the acquisition of 10,000 events.

2.4. DNA fragmentation analysis

DNA was extracted from a colon epithelial cell line. In brief, cells (2×10^6) in PBS were centrifuged for 5 min ($400 \times g$) at 4 °C, and the pellet was suspended in 0.1 ml hypotonic lysis buffer (10 mM Tris, pH 7.4, 10 mM EDTA, pH 8.0, 0.5% (v/v) Triton X-100). Cells were incubated for 15 min at 4 °C. The resultant lysate was centrifuged for 30 min ($17{,}019 \times g$) at 4 °C. The supernatant containing fragmented DNA was digested for 1 h at 37 °C with 0.04 mg/ml of RNase A (Bio Basic Inc., Ontario, Canada) and then incubated for an additional 1 h at the same temperature with 0.04 mg/ml of proteinase K (Sigma). DNA was precipitated in 50% (v/v) isopropanol in 0.4 M NaCl at −20 °C overnight. The precipitate was centrifuged at 13,000 rpm for 30 min at 4 °C. The resultant pellet was air dried and re-suspended in TE Buffer. An aliquot equivalent to 2×10^6 cells was electrophoresed at 40 V for 3 h in a 2% (w/v) agarose gel in 90 mM Tris–glacial acetic acid buffer containing 2 mM EDTA (pH 8.0). After electrophoresis, the gel was stained with ethidium bromide (1 μg/ml), and the nucleic acids were visualized with a UV transilluminator. A 1 kb + DNA ladder (SolGent Co., Ltd., Korea) was used for molecular sizing.

2.5. Construction of plasmids

A CMV-driven small interference RNA (siRNA) expression vector was constructed by inserting a hairpin siRNA (shRNA) template into the *pSilencer 4.1-CMV-neo* vector (Ambion Inc., Austin, TX, USA). The empty vector and EGR-1 shRNA insert-

containing vector were named as pSilence and pSiEGR1, respectively. Insert Egr-1 siRNA (Dharmacon, Lafayette, CO, USA) was targeting the sequence, AAGTTACTACCTC TTATCCAT. Sense ATF-3 cDNA expression plasmid (pScATF3) and ATF-3 antisense expression plasmid (pAsATF3) were generously provided by Frank Buttone and Thomas Eling (NIEHS/NIH, NC, USA). The procedure for constructing the plasmids can be briefly as follows: a construct containing the entire coding region of ATF-3 including the TATAA region was generated by RT-PCR using RNA from HCT-116 cells with the following primers: forward CGTGAGTCCTCGGTGCTC and reverse GACAGCTCTCCAATGGCTTC. The resulting 721 bp construct was cloned into pCRII-Topo (Invitrogen, Carlsbad, CA, USA) followed by excision at the HindIII/NotI sites, transferred in the sense and antisense orientations into the expression plasmid pcDNA3.1Zeo+/− (Invitrogen) using T4 DNA ligase (NEB, Beverly, MA, USA) and then confirmed by DNA sequencing. MIC-1 shRNA expression vector and luciferase promoter (−133/+70) reporter plasmid were kindly provided by Dr. Jong-Sik Kim (Andong National University, Korea) and Dr. Seong-Joon Baek (The University of Tennessee, USA).

2.6. Western immunoblot analysis

Levels of protein expression were compared using Western immunoblot analysis. This was conducted using rabbit polyclonal anti-p21 and anti-human actin antibody (Santa cruz Biotechnology, Santa Cruz, CA, USA), rabbit polyclonal anti-p-ERK and anti-p-AKT antibody (Cell Signaling Technology, Beverly, MA, USA). Cells were washed with ice-cold phosphate buffer, lysed in boiling lysis buffer [1% (w/v) SDS, 1.0 mM sodium ortho-vanadate, and 10 mM Tris, pH 7.4], and sonicated for 5 s. Lysates containing proteins were quantified using BCA protein assay kit (Pierce, Rockford, IL, USA). Fifty micrograms of protein were separated by Bio-Rad gel mini electrophoresis. The proteins were transferred onto a PVDF membrane (Amersham Pharmacia Biotech, Piscataway, NJ, USA) and the blots were blocked for 1 h with 5% skim milk in Tris-buffered saline plus Tween 0.05% (TBST) and then probed with each antibody for 2 h at room temperature or overnight at 4 °C. After washing three times with TBST, the blots were incubated with horseradish-conjugated secondary antibody for 1 h and then washed with TBST three times. Protein was detected using ECL Chemiluminescent substrate (Amersham Pharmacia Biotech, Piscataway, NJ, USA).

2.6.1. Traditional reverse transcription-polymerase chain reaction (RT-PCR)

RNA was extracted with the RNeasy kit (Qiagen, Valencia, CA, USA) according to the manufacturer's instructions. RNA (100 ng) from each sample was transcribed to cDNA by BD Sprint PowerScript (Clontech, Mountain View, CA, USA). The amplification was performed with Takara HS ExTaq DNA Polymerase (Takara Bio Inc., Shiga, Japan) in a *Mycycler* Thermal Cycler (Bio-Rad Laboratories Inc., Hercules, CA, USA) using the following parameters; denaturation at 94 °C for 2 min and 25 cycles of denaturation at 98 °C for 10 s, annealing at 59 °C for 30 s, and elongation at 72 °C for 45 s. An aliquot of each PCR product was subjected to 1.2% (w/v) agarose gel electrophoresis and visualized by staining with ethidium bromide. The 5′ forward and 3′ reverse-complement PCR primers for amplification of each gene were as follow: human urokinase-type plasminogen activator receptor (uPAR 5′-GCC TTA CCG AGG TTG TGT GT-3′ and 5′-GGC AGA TTT TCA AGC TCC AG-3′), human urokinase-type plasminogen activator (PLAU, 5′-GCC ATC CCG GAC TAT ACA GA-3′ and 5′-AGG CCA TTC TCT TCC TTG GT-3′), human EGR-1 (5′-CAG TGG CCT AGT GAG CAT GA-3′ and 5′-CCG CAA GTG GAT CTT GGT AT-3′), human ATF-3 (5′-GAT CTA GAG CAG TCG TGG TAT GG-3′ and 5′-GAT CTA GAT TTA CCA TGT CTT GG-3′), and human GAPDH (5′-TCA ACG GAT TTG GTC GTA TT-3′ and 5′-CTG TGG TCA TGA GTC CTT CC-3′).

2.7. Fluorescence staining protocol

Fluorescence microscopy was performed according to the following methods. Cells were fixed with 3.7% paraformaldehyde in PBS for 15 min. After two washes with PBS, cells were permeabilized with 0.2% Triton X-100 for 3–5 min at room temperature. After three washes with PBS, cells were stained with 1 μg/ml FITC-labeled phalloidin for 20 min at room temperature and washed with PBS three times. The stained cells were mounted in Cytoseal reagent before observation under the fluorescence microscope (Olympus IX70, Tokyo, Japan).

2.8. Transfection and luciferase assay

Cells were transfected with a mixture of plasmids using Trans-LT1 transfection reagent (Mirus, Madison, WI, USA) according to the manufacturer's protocol. MIC-1 shRNA expression vector (pSiMIC1) construct was co-transfected with pcDNA3.1-neo. Following transfection, cells underwent 2 weeks of selection with 400 μg/ml G418 (Life Technologies). Single colonies were expanded and maintained in medium with 200 μg/ml G418. For transfection of the luciferase reporter gene, a mixture of 1.5 μg firefly luciferase reporter, 0.15 μg renilla luciferase, and pRL-null vector (Promega, Madison, WI, USA) per 4.5 μl of Trans-LT1 reagent was added to a 6-well culture plate. For the luciferase assay, 18 h after transfection, the cells were exposed to chemicals for the next 24 h and lysed for dual-luciferase reporter assay system (Promega, Madison, WI, USA). All tranfection efficiencies were maintained at around 50–60%, which was confirmed with pMX-enhanced GFP vector. To measure luciferase activity, cells were washed with cold PBS, lysed with passive lysis buffer (Promega) and then centrifuged at 12,000 × *g* for 4 min. The supernatant was collected isolated and stored at −80 °C until assessment of the luciferase activity. The luciferase activity was measured with a dual-mode luminometer (Model TD-20/20, Turner Designs Co., Sunnyvale, CA, USA) after briefly mixing the supernatant (10 μl) with 50 μl *firefly* luciferase assay substrate solution, followed with 50 μl stopping *renilla* luciferase assay solution (Promega). The *firefly* luciferase activity was related to the *renilla* luciferase activity to get relative luciferase units (RLU).

2.9. Statistical analyses

Data were analyzed using SigmaStat for Windows (Jandel Scientific, San Rafael, CA, USA). For comparative analysis, Student's *t*-test was performed. For the multi-factorial analysis, data were subjected to Analysis of Variance (ANOVA) and pairwise comparisons according to the Student–Newman–Keuls (SNK) method. Data not meeting normality assumptions were subjected to Kruskal–Wallace ANOVA on ranks and then pairwise comparisons made by the SNK method.

3. Results

3.1. Ribotoxic anisomycin induced tumor cell apoptosis mediated by MIC-1 protein

We tested the effects of anisomycin on the cell growth of human colon carcinoma HCT-116 cells; this cell line has been extensively investigated as a representative model of human colon cancer in culture [34,35]. Several studies have demonstrated that the ribotoxic stress agent anisomycin can suppress malignant tumor cell growth [17,19]. In this study, it was investigated

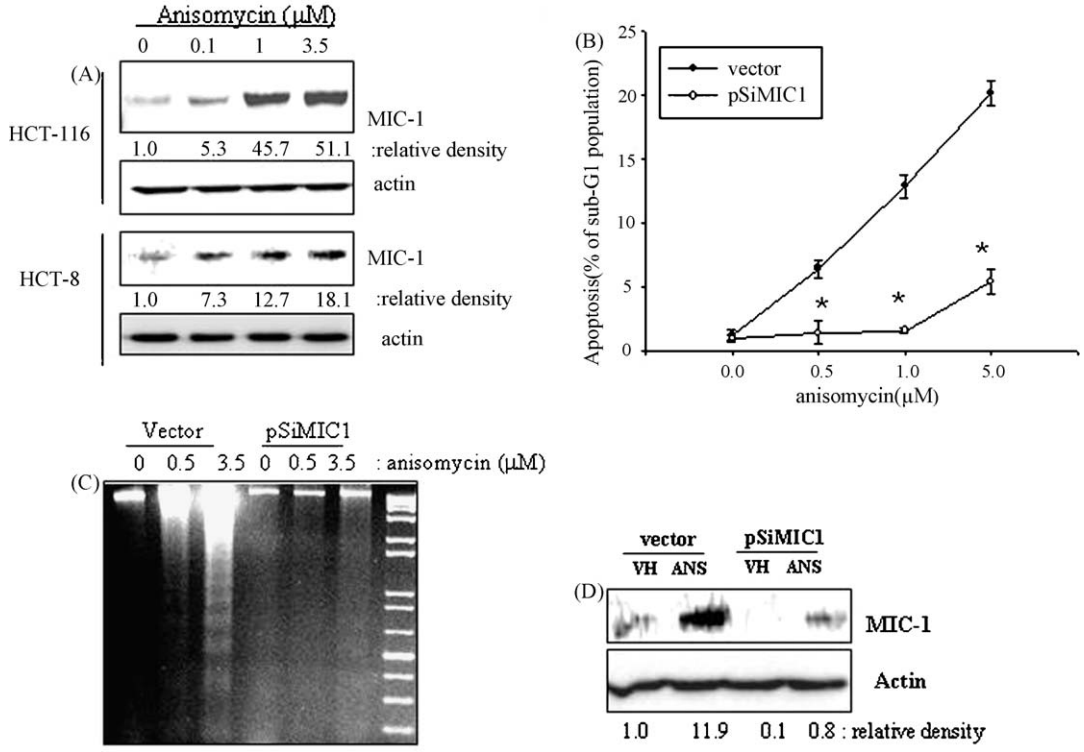

Fig. 1. Involvement of MIC-1 in anisomycin-induced apoptosis. (A) HCT-116 and HCT-8 cells were treated with anisomycin for 24 h. Total protein was analyzed using Western blot analysis. (B) Vector- or pSiMIC1-transfected HCT-116 cells were each treated with a dose of anisomycin for 48 h and then cells were stained for FACS analysis. The marker '*' indicates a significant difference from anisomycin-treated vector-transfected cells ($p < 0.05$). (C) Vector- or pSiMIC1-transfected HCT-116 cells were each treated with a dose of anisomycin for 9 h and then the cellular fragmented DNA was analyzed. (D) Vector- or pSiMIC1-transfected HCT-116 cells were treated with vehicle (VH) or 1 μM anisomycin (ANS) for 24 h and the total cell lysate was analyzed using Western blot analysis. Results are representative of three independent experiments.

whether tumor-associated protein MIC-1 was influenced by the ribotoxic stress. Treatment with anisomycin (ANS) enhanced MIC-1 protein expression dose-dependently in the human colon carcinoma (HCT-116) and ilocecal cancer cells (HCT-8) (Fig. 1A). Anisomycin also triggered apoptotic death of the colon cancer cells in a dose-dependent way (Fig. 1B). Since MIC-1 protein is known to play critical roles in tumor cell regulation, we tested whether the protein was also involved in the ribotoxic stress-induced responses in the colon cancer cells. Genetic suppression of MIC-1 expression by shRNA expression attenuated the ribotoxin-induced apoptotic cell death, suggesting a positive association between MIC-1 protein and the anisomycin-induced cell death (Fig. 1B). This apoptotic pattern was similarly demonstrated with the DNA fragmentation assay (Fig. 1C). Anisomycin-induced MIC-1 protein which was interfered by stable expression of MIC-1 shRNA in the human colon cancer cells (Fig. 1D).

3.2. MIC-1 triggered the gene expression of the urokinase-type plasminogen activator (PLAU) and its receptor (PAR) in the presence of the ribotoxic agent

Among the MIC-1-induced gene products, up-regulation of the urokinase-type plasminogen activator (PLAU) system was observed with the study of anisomycin treatment using microarray analysis (data not shown). Anisomycin increased the gene expression of PLAU and uPAR in the colon carcinoma HCT-116 cells and each induction reached maximal level at about 9–12 h post-treatment, which was later than the MIC-1 maximal induction time (4 h post-treatment) (Fig. 2A). When cellular MIC-1 induction was interfered with using MIC-1 shRNA expression, anisomycin-induced PLAU and uPAR expression were also attenuated (Fig. 2B). Therefore MIC-1 appears to be an important modulator of PLAU and uPAR expression in the presence of ribotoxic anisomycin. However, it is also possible that PLAU system can be triggered by ribotoxic stress independently of MIC-1 protein. From the early part of this study, it was found that MIC-1 was a positive regulator of ribotoxin-induced apoptosis. Thus MIC-1-modulated PLAU/uPAR expression was tested for its effects on the anisomycin-induced apoptosis. Suppression of PLAU/uPAR activity with specific urokinase inhibitor amiloride reduced the programmed cell death, suggesting that the ribotoxin-induced apoptotic cell death was mediated by PLAU system as well as MIC-1 (Fig. 2C).

On the assumption that increased cell death was due to the suppressed cellular survival, mitogenic signaling activation was assessed. We investigated the effects of ribotoxin-mediated stress on the key survival-related signaling molecules such as phosphorylated ERK and AKT. Suppression of MIC-1 induction enhanced the ribotoxin-activated ERK1 phosphorylation. Moreover, MIC-1-interfered cells showed increased levels of phospho-AKT in the presence of ribotoxin anisomycin (Fig. 3A). Blocking of PLAU/uPAR action with specific urokinase inhibitor also enhanced the survival signals ERK1 phosphorylation in the colon cancer cells (Fig. 3B). However, direct inhibition of ERK signals by U0126 reduced HCT-116 carcinoma cellular viability in presence of anisomycin, suggesting positive association between ERK signals and tumor cell survival response to the ribotoxic stress (Fig. 3C). Taken together, MIC-1 mediated the induction of the urokinase-type plasminogen activator (PLAU) and its receptor (PAR). When the apoptotic pathways via MIC-1 or PLAU/uPAR induction were repressed, cell survival signals were enhanced by the ribotoxic stress agent in the cancer cells.

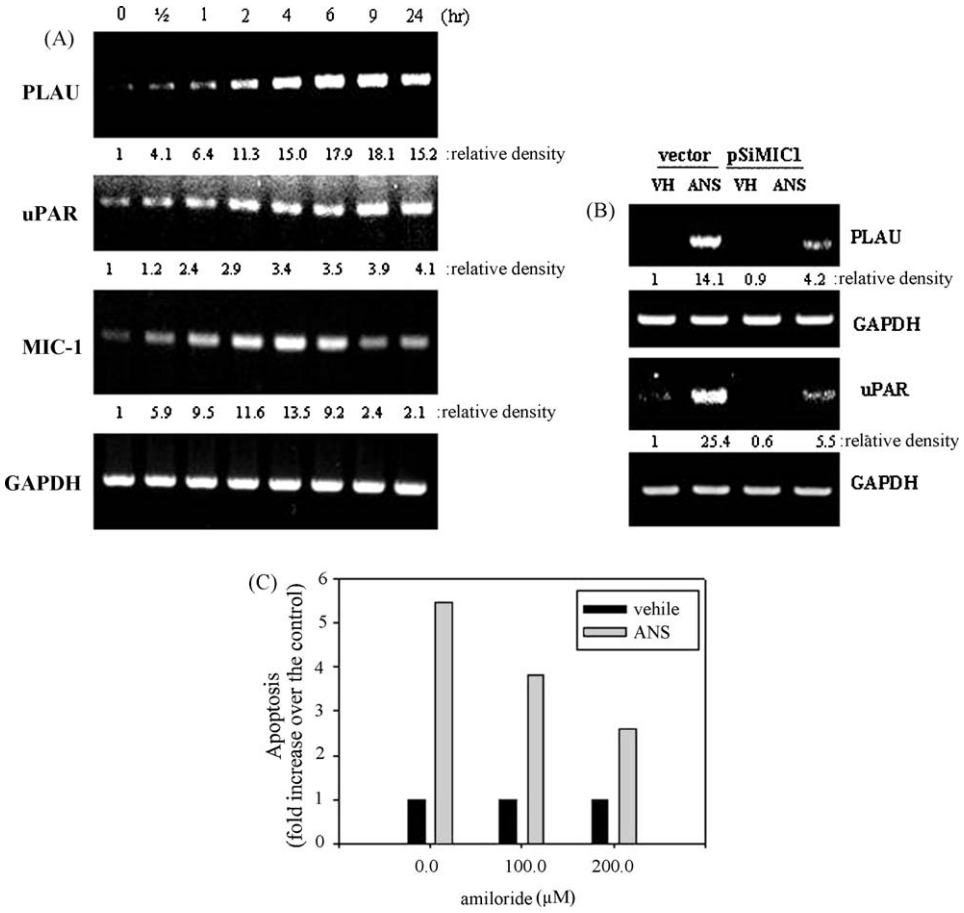

Fig. 2. Involvement of PLAU system in anisomycin-induced apoptosis. (A) HCT-116 cells were treated with 1 μM anisomycin for the indicated period of time. Total RNA was analyzed using RT-PCR methodology. (B) Vector- or pSiMIC1-transfected HCT-116 cells were treated with 1 μM anisomycin for 9 h and then total RNA was analyzed using RT-PCR. (C) HCT-116 cells were each treated with a dose of urokinase inhibitor (amiloride) in the presence of anisomycin (ANS) and then cells were stained for FACS analysis. All results are representative of three independent experiments.

3.3. Ribotoxic anisomycin-induced MIC-1 gene expression mediated by p38 MAP kinase and its immediate gene product ATF-3

To address the signaling mechanism of MIC-1 induction by ribotoxic anisomycin, we studied the immediate responsive transcription factors such as EGR-1 and ATF-3 that have been extensively investigated for MIC-1 gene induction [36–38]. Anisomycin elevated ATF-3 and EGR-1 expression, and the peak of each gene expression was earlier than that of MIC-1 gene expression (Fig. 4A). To test whether ATF-3 or EGR-1 activation was involved in MIC-1 transcription, the effect of genetic suppression or induction of these transcription factors was assessed by measuring the MIC-1 reporter luciferase activity. EGR-1 shRNA expression did not significantly alter anisomycin-induced MIC-1 protein and promoter activation (data not shown). By contrast, ATF-3-overexpression enhanced anisomycin-induced MIC-1 transcriptional activity, while antisense ATF-3 slightly suppressed the activation (Fig. 4B). These results suggest that anisomycin-induced ATF-3 mediated MIC-1 transcriptional activation. MIC-1 protein levels were compared among the ATF-3 sense-, antisense-, or empty vector-transfected cells in response to anisomycin treatment. Antisense ATF-3 strongly attenuated MIC-1 protein expression which suggested positive regulation of MIC-1 by ATF-3 in the presence of ribotoxic anisomycin (Fig. 4C).

Since ribotoxic stresses trigger early stress signaling pathways such as MAP kinase or PI3 kinase, several signaling kinase inhibitors (U0126 [a specific MEK1/2 inhibitor], SP600125 [JNK inhibitor], SB203580 [p38 MAP kinase inhibitor], or LY294002 [PI3 kinase inhibitor]) were compared for their effect on anisomycin-induced MIC-1 gene expression. Among these, only p38 MAP kinase inhibition attenuated anisomycin-induced MIC-1 expression (Fig. 5A). Anisomycin increased phosphorylation of p38 MAP kinase, which has also been previously reported (Fig. 5C) [23,39]. Activated p38 MAP kinase was shown to mediate anisomycin-induced ATF-3 gene expression as well as MIC-1 protein (Fig. 5A and B) since p38 was activated by anisomycin (Fig. 5C). However, we cannot exclude the possibility of ATF-3-independent MIC-1 induction via the p38 MAP kinase signaling pathway. Subsequently, the molecular mechanism of p38-mediated MIC-1 induction was further investigated.

At the transcriptional level, p38 MAP kinase inhibition was demonstrated to partly reduce anisomycin-induced MIC-1 promoter activity (Fig. 5D). In addition to the effects on the promoter activity, we tested the contribution of post-transcriptional regulation to MIC-1 induction by anisomycin, since MAP kinase signaling cascades are known to alter mRNA stability of particular genes [25,40]. Anisomycin treatment extended the MIC-1 mRNA half-life while p38 MAP kinase inhibition diminished the anisomycin-extended half-life of MIC-1 mRNA in HCT-116 cells (Fig. 6E). Therefore, anisomycin activated p38 MAP kinase signaling cascade, which mediated MIC-1 expression both transcriptionally and post-transcriptionally.

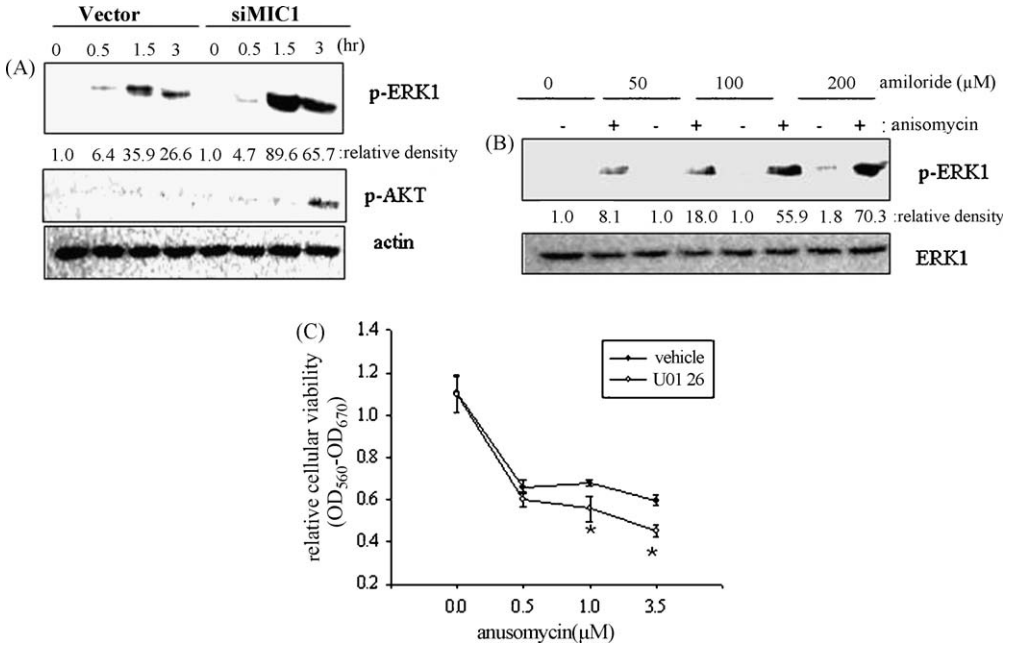

Fig. 3. Effect of MIC-1 and PLAU inhibition on the survival signals. (A) Vector- or psiMIC1-transfected HCT-116 cells were treated with vehicle (VH) or 1 μM anisomycin (ANS) for 24 h and the total cell lysate was analyzed using Western blot analysis. (B) HCT-116 cells were treated with each combination of chemicals (anisomycin and amiloride) and the total cell lysate was analyzed using Western blot analysis. (C) HCT-116 cells were treated with vehicle (VH) or 1 μM anisomycin (ANS) in presence of 500 nM U0126. Cellular viability was analyzed using MTT assay. Results are representative of three independent experiments. The marker '*' indicates a significant difference from the vehicle group at each dose of anisomycin ($p < 0.05$).

4. Discussion

Ribotoxic stress anisomycin induced cellular apoptosis which was associated with MIC-1 induction in the colon cancer cells. It has been known that xenobiotic-induced and constitutive expression of MIC-1 protein led to G1 or S phase cell cycle arrest as well as apoptosis in the cancer cells [41,42]. Although the mechanism of MIC-1-mediated cell death is not clearly understood, several explanations have been reported. Evidences suggest that MIC-1 can mediate p53-dependent growth suppression since the promoter of MIC-1 has a potential regulatory site for p53 binding [6,42,43]. However, MIC-1 can induce apoptotic death in cells deficient in p53, suggesting a p53-independent pathway for MIC-1 activity [44]. The results of our study demonstrated that MIC-1-linked urokinase PLAU was involved in the ribotoxic stress-induced tumor cell apoptosis. However, several reports demonstrate that the PLAU/uPAR system protects cells from apoptotic cell death in the normal tissues or the non-transformed epithelial cells

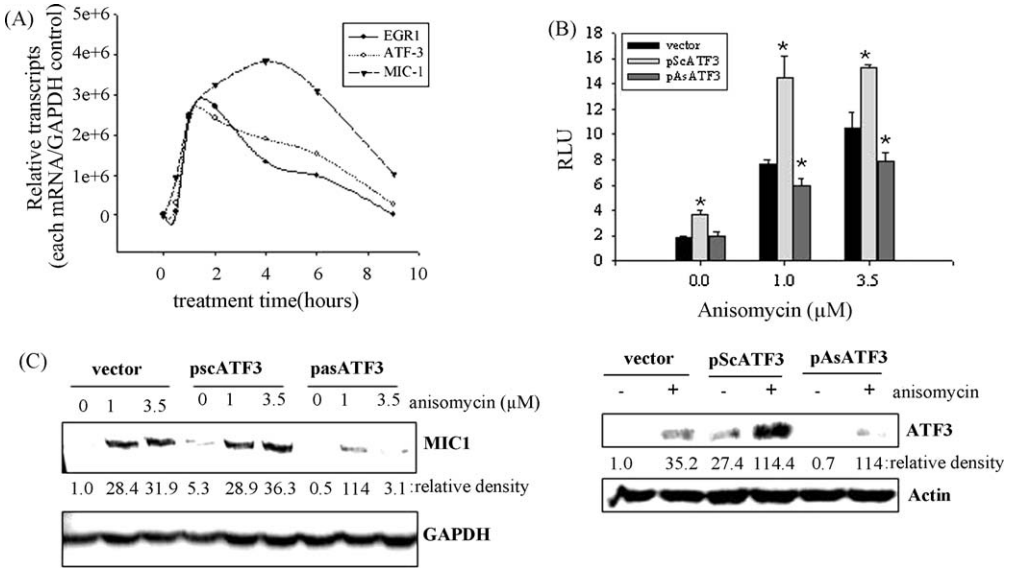

Fig. 4. Effects of ATF-3 on anisomycin-induced MIC-1 expression. (A) HCT-116 cells were treated with 1 μM anisomycin for the indicated time periods. Relative mRNA levels were compared using RT-PCR. (B) HCT-116 cells were transfected with vector, sense ATF-3 (pScATF3) or antisense ATF-3 expression plasmid (pAsATF3) in presence of MIC-1 promoter reporter plasmid. After transfection, cells were treated with anisomycin for 24 h and then the luciferase activity was measured. The marker '*' indicates a significant difference from vector-transfected group at each dose of anisomycin ($p < 0.05$). B (box) and (C) HCT-116 cells were transfected with vector, sense ATF-3 or antisense ATF-3 expression plasmid. Then, 24 h after transfection, cells were treated with anisomycin for 4 or 24 h, respectively and then ATF-3 or MIC-1 protein was measured. Results are representative of three independent experiments.

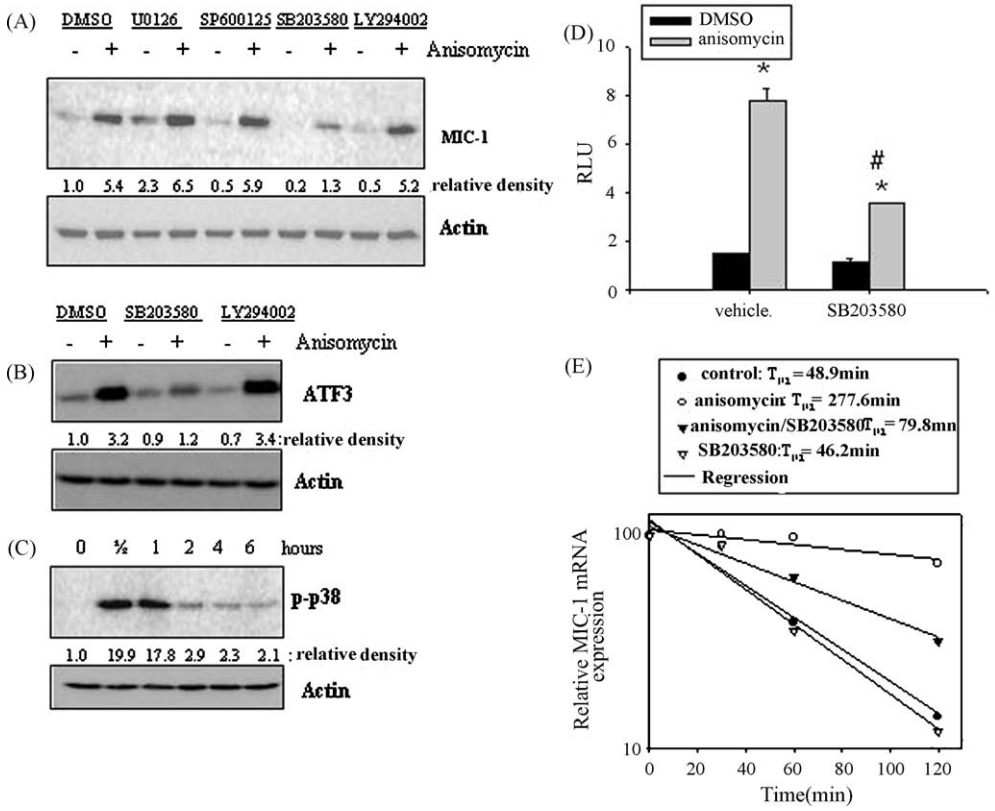

Fig. 5. Involvement of p38 MAP kinase in ATF-3 and MIC-1 induction. (A) HCT-116 cells were co-treated with DMSO or each kinase inhibitor (10 μM U0126 [a specific MEK1/2 inhibitor], 5 μM SP600125 [JNK inhibitor], 5 μM SB203580 [p38 MAP kinase inhibitor], or 5 μM LY294002 [PI3 kinase inhibitor]) in the presence of 1 μM anisomycin for 24 h. Total cell lysates were subjected to Western blot analysis. (B) HCT-116 cells were pre-treated with DMSO or each kinase inhibitor (5 μM SB203580 [p38 MAP kinase inhibitor], or 5 μM LY294002 [PI3 kinase inhibitor]) and then treated with 1 μM anisomycin for 4 h. The total cell lysates were subjected to Western blot analysis. (C) HCT-116 cells were incubated in the presence of 1 μM anisomycin for a given time and the total cell lysates were subjected to Western blot analysis. (D) HCT-116 cells were transfected with the MIC-1 promoter reporter plasmid. After transfection, cells were treated with 1 μM anisomycin plus vehicle or inhibitor for 24 h and then the luciferase activity was measured. The marker '*' indicates a significant difference from vehicle DMSO group ($p < 0.05$). The marker '#' indicates a significant difference from anisomycin-treatment group without inhibitor ($p < 0.05$). (E) HCT-116 cells were treated with 1 μM anisomycin for 4 h to reach the maximum level and then transcription was terminated by adding 5 μM actinomycin D in the presence of the vehicle or inhibitors (5 μM SB203580). Total RNA was analyzed using RT-PCR. Results are representative of three independent experiments.

[29,45]. These prior studies showed that PLAU activates the survival pathways such as ERK and AKT signaling pathways in response to the cytotoxic injuries [46]. By contrast, recent studies have shown that the pro-apoptotic actions of PLAU/uPAR in the metastatic tumor cells as well as normal cells by blocking survival signals [47–49]. Pro-apoptotic pathways require mitochondria-dependent mechanisms, and BAD protein serves as a downstream molecule depending on the nature of the cellular interaction [48]. MIC-1 suppression or inhibition of PLAU action, in the context of the ribotoxic stress, enhanced the survival signaling pathways including ERK activation, suggesting that MIC-1-associated stimulation may suppress the cell survival responses to the ribotoxic stress. However, since ERK inhibition partially reduced anisomycin-induced cytotoxicity in Fig. 3C, there could be a redundancy in the survival response signals. Therefore, it is warranted to address additional survival signaling factors involved in ribotoxic responses in the future study.

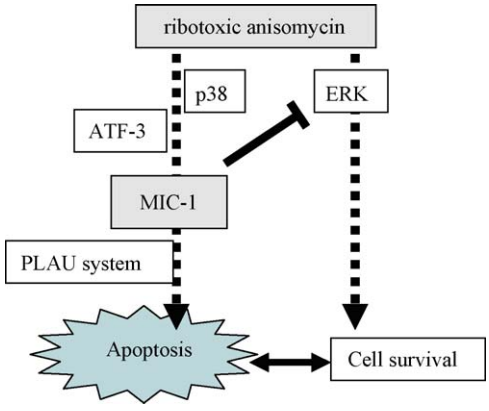

Fig. 6. A putative mechanism of ribotoxic stress agent-mediated MIC-1 induction and its role in the colon cancer cells. The schematic signaling patterns illustrate that chemical ribotoxic stress-induced MIC-1 protein and PLAU system are modulated. Ribotoxic agents activate p38 MAP kinase signals and ERK signaling cascade. p38 MAP kinase can increase ATF-3 and MIC-1. MIC-1 expression is also followed by apoptosis-promoting PLAU/uPAR. However, ERK signal is associated with cell survival after the ribotoxic insult. This survival process can promote tumor cell survival when exposed to the anti-cancer ribotoxic agents.

The results of this study showed that the early responsive gene product ATF-3 mediated MIC-1 production at the transcriptional level. ATF-3 is a transcription factor of the ATF/cyclic AMP response element-binding family that contains a basic region/leucine zipper DNA-binding motif and binds to the cyclic AMP response element consensus sequence [50]. ATF-3 is regarded as an adaptive responsive factor in addition to an immediately induced stress-activated gene product [51]. In terms of cancer development, ATF-3 as a stress-inducible gene promotes cellular apoptosis and cell cycle arrest in untransformed and benign tumor cells. In response to the acute therapeutic stress, activated ATF-3 suppresses tumorigenesis depending on the tissue types and cancer environmental texture [52,53]. However, ATF-3 has also been known to enhance tumor progression by up-regulating genes involved in

tumor metastasis and is considered advantageous for the malignant cancer cells [54]. Using a breast cancer model, it was shown that ATF-3 levels were elevated in about 50% of tumors, which supports the dichotomous roles of ATF-3 in tumor progression. Many chemotherapeutic agents such as NSAIDs, adriamycin, the PI3 kinase inhibitor LY294002, and various phytochemicals have been reported to induce ATF-3 protein [53,55,56]. Since ATF-3 has oncogenic potential, these anti-cancer agents might result in adverse effects by elevating ATF-3 and thus more careful risk evaluations are required for their treatment. Similar to ATF-3, MIC-1 has dichotomous activity in tumor progression depending on the maturity of the protein and the malignancy of the tumor. In addition to the MIC-1-induced apoptosis in response to the chemotherapeutic agents, patients with metastatic epithelial cancer show elevated MIC-1 expression within the tumor tissue as well as the serum MIC-1 levels [57]. For the late stage tumors, MIC-1 may be involved in tumor metastasis, and high serum levels of mature type MIC-1 may lead to other pro-carcinogenic systemic effects. Therefore, further investigation of the chronic action of MIC-1 induction, in normal and transformed intestinal epithelial cells, is needed although the acutely produced MIC-1 caused apoptotic cell death in the colon carcinoma cells.

At the post-transcriptional level, our results indicate that anisomycin elevated MIC-1 mRNA stability via the p38 MAP kinase pathway. The enhanced mRNA half-life has been studied previously in many investigations on ribotoxic stress [40,58–60]. Several reports have also demonstrated that MIC-1 mRNA is modulated at the post-transcriptional level since the 3′-untranslated region of MIC-1 has four copies of AU rich elements (ARE) that could determine mRNA stability [61–63]. Moreover, activated MAP kinase signaling cascades such as the p38 MAP kinase critically contribute to high levels of protein expression of genes that have ARE sequences [25,58]. How the MAP kinase pathway regulates MIC-1 mRNA stability remains to be determined. RNA stability can be regulated by various factors such as the protection of the 3′-untranslated region of MIC-1 transcripts by RNA-binding proteins. Among the RNA-binding proteins, HuR which promotes mRNA stabilization, has been shown to be involved in PLAU mRNA stability [64]. Ribotoxic stress by UV irradiation is also mediated by ERK1/2 MAP kinase activation to elicit HuR-regulated mRNA stabilization [65,66]. Moreover, tristetraprolin, a decay-promoting RNA-binding protein, has been shown to act in an MAP kinase-dependent manner in order to regulate the stability of its own mRNA [67] and may likewise influence MIC-1 mRNA stability. Ribotoxic deoxynivalenol has been shown to elevate cyclooxygenase mRNA half-life by the p38 MAP kinase signaling pathway, which is linked to the modulation of AU rich elements at the 3′-untranslated region [25]. In the present study, the p38 MAP kinase signaling pathway played an important role in MIC-1 RNA stabilization in human colon cancer cells. It is thus warranted to further investigate the molecular mechanism of the ribotoxic stress-induced MIC-1 mRNA stability in terms of interaction with RNA-binding proteins via p38 MAP kinase activation.

Taken in sum, ribosome-inactivating chemical stress-induced MIC-1 expression both at the transcriptional and post-transcriptional levels and subsequent apoptosis-modulating gene production was enhanced while suppressing survival ERK signals in the colon cancer cells (Fig. 6). The results of this study provide mechanistic insight into the tumor cell decision for death or survival in response to the chemotherapeutic ribotoxic stresses.

Acknowledgement

This work was supported by the Korea Research Foundation (KRF) grant funded by the Korea government (MEST) (No. 2009-0065479).

References

[1] Brown DA, Ward RL, Buckhaults P, Liu T, Romans KE, Hawkins NJ, et al. MIC-1 serum level and genotype: associations with progress and prognosis of colorectal carcinoma. Clin Cancer Res 2003;9(7):2642–50.
[2] Johnen H, Lin S, Kuffner T, Brown DA, Tsai VW, Bauskin AR, et al. Tumor-induced anorexia and weight loss are mediated by the TGF-beta superfamily cytokine MIC-1. Nat Med 2007;13(11):1333–40.
[3] Nakamura T, Scorilas A, Stephan C, Yousef GM, Kristiansen G, Jung K, et al. Quantitative analysis of macrophage inhibitory cytokine-1 (MIC-1) gene expression in human prostatic tissues. Br J Cancer 2003;88(7):1101–4.
[4] Baek SJ, Wilson LC, Lee CH, Eling TE. Dual function of nonsteroidal anti-inflammatory drugs (NSAIDs): inhibition of cyclooxygenase and induction of NSAID-activated gene. J Pharmacol Exp Ther 2002;301(3):1126–31.
[5] Okazaki R, Moon Y, Norimura T, Eling T. Ionizing radiation enhances the expression of the nonsteroidal anti-inflammatory drug-activated gene (NAG1) by increasing the expression of TP53 in human colon cancer cells. Radiat Res 2006;165(2):125–30.
[6] Lim JH, Park JW, Min DS, Chang JS, Lee YH, Park YB, et al. NAG-1 up-regulation mediated by EGR-1 and p53 is critical for quercetin-induced apoptosis in HCT116 colon carcinoma cells. Apoptosis 2007;12(2):411–21.
[7] Shim M, Eling TE. Protein kinase C-dependent regulation of NAG-1/placental bone morphogenic protein/MIC-1 expression in LNCaP prostate carcinoma cells. J Biol Chem 2005;280(19):18636–42.
[8] Wilson LC, Baek SJ, Call A, Eling TE. Nonsteroidal anti-inflammatory drug-activated gene (NAG-1) is induced by genistein through the expression of p53 in colorectal cancer cells. Int J Cancer 2003;105(6):747–53.
[9] Gray JS, Bae HK, Li JC, Lau AS, Pestka JJ. Double-stranded RNA-activated protein kinase mediates induction of interleukin-8 expression by deoxynivalenol, Shiga toxin 1, and ricin in monocytes. Toxicol Sci 2008;105(2):322–30.
[10] Jandhyala DM, Ahluwalia A, Obrig T, Thorpe CM. ZAK: a MAP3Kinase that transduces Shiga toxin- and ricin-induced proinflammatory cytokine expression. Cell Microbiol 2008;10(7):1468–77.
[11] Shifrin VI, Anderson P. Trichothecene mycotoxins trigger a ribotoxic stress response that activates c-Jun N-terminal kinase and p38 mitogen-activated protein kinase and induces apoptosis. J Biol Chem 1999;274(20):13985–92.
[12] Barbacid M, Vazquez D. Ribosome changes during translation. J Mol Biol 1975;93(4):449–63.
[13] Bunyard P, Handley M, Pollara G, Rutault K, Wood I, Chaudry M, et al. Ribotoxic stress activates p38 and JNK kinases and modulates the antigen-presenting activity of dendritic cells. Mol Immunol 2003;39(13):13–21.
[14] Instanes C, Hetland G. Deoxynivalenol (DON) is toxic to human colonic, lung and monocytic cell lines, but does not increase the IgE response in a mouse model for allergy. Toxicology 2004;204(1):13–21.
[15] Smith WE, Kane AV, Campbell ST, Acheson DW, Cochran BH, Thorpe CM. Shiga toxin 1 triggers a ribotoxic stress response leading to p38 and JNK activation and induction of apoptosis in intestinal epithelial cells. Infect Immun 2003;71(3):1497–504.
[16] Ruller S, Stahl C, Kohler G, Eickhoff B, Breder J, Schlaak M, et al. Sensitization of tumor cells to ribotoxic stress-induced apoptotic cell death: a new therapeutic strategy. Clin Cancer Res 1999;5(10):2714–25.
[17] Xia S, Li Y, Rosen EM, Laterra J. Ribotoxic stress sensitizes glioblastoma cells to death receptor induced apoptosis: requirements for c-Jun NH2-terminal kinase and Bim. Mol Cancer Res 2007;5(8):783–92.
[18] Rennebeck G, Martelli M, Kyprianou N. Anoikis and survival connections in the tumor microenvironment: is there a role in prostate cancer metastasis? Cancer Res 2005;65(24):11230–5.
[19] Mawji IA, Simpson CD, Gronda M, Williams MA, Hurren R, Henderson CJ, et al. A chemical screen identifies anisomycin as an anoikis sensitizer that functions by decreasing FLIP protein synthesis. Cancer Res 2007;67(17):8307–15.
[20] Abayasiriwardana KS, Barbone D, Kim KU, Vivo C, Lee KK, Dansen TB, et al. Malignant mesothelioma cells are rapidly sensitized to TRAIL-induced apoptosis by low-dose anisomycin via Bim. Mol Cancer Ther 2007;6(10):2766–76.
[21] Curtin JF, Cotter TG. Anisomycin activates JNK and sensitises DU 145 prostate carcinoma cells to Fas mediated apoptosis. Br J Cancer 2002;87(10):1188–94.
[22] Cano E, Hazzalin CA, Mahadevan LC. Anisomycin-activated protein kinases p45 and p55 but not mitogen-activated protein kinases ERK-1 and -2 are implicated in the induction of c-fos and c-jun. Mol Cell Biol 1994;14(11):7352–62.
[23] Hazzalin CA, Le Panse R, Cano E, Mahadevan LC. Anisomycin selectively desensitizes signalling components involved in stress kinase activation and fos and jun induction. Mol Cell Biol 1998;18(4):1844–54.
[24] Zinck R, Cahill MA, Kracht M, Sachsenmaier C, Hipskind RA, Nordheim A. Protein synthesis inhibitors reveal differential regulation of mitogen-activated protein kinase and stress-activated protein kinase pathways that converge on Elk-1. Mol Cell Biol 1995;15(9):4930–8.
[25] Moon Y, Pestka JJ. Vomitoxin-induced cyclooxygenase-2 gene expression in macrophages mediated by activation of ERK and p38 but not JNK mitogen-activated protein kinases. Toxicol Sci 2002;69(2):373–82.
[26] Ouyang DY, Wang YY, Zheng YT. Activation of c-Jun N-terminal kinases by ribotoxic stresses. Cell Mol Immunol 2005;2(6):419–25.
[27] Lu D, Chen J, Hai T. The regulation of ATF3 gene expression by mitogen-activated protein kinases. Biochem J 2007;401(2):559–67.
[28] Moon Y, Yang H, Lee SH. Modulation of early growth response gene 1 and interleukin-8 expression by ribotoxin deoxynivalenol (vomitoxin) via ERK1/2

in human epithelial intestine 407 cells. Biochem Biophys Res Commun 2007;362(2):256–62.
[29] Hildenbrand R, Gandhari M, Stroebel P, Marx A, Allgayer H, Arens N. The urokinase-system—role of cell proliferation and apoptosis. Histol Histopathol 2008;23(2):227–36.
[30] Crippa MP. Urokinase-type plasminogen activator. Int J Biochem Cell Biol 2007;39(4):690–4.
[31] Mazzieri R, Furlan F, D'Alessio S, Zonari E, Talotta F, Verde P, et al. A direct link between expression of urokinase plasminogen activator receptor, growth rate and oncogenic transformation in mouse embryonic fibroblasts. Oncogene 2007;26(5):725–32.
[32] Lee DH, Yang Y, Lee SJ, Kim KY, Koo TH, Shin SM, et al. Macrophage inhibitory cytokine-1 induces the invasiveness of gastric cancer cells by up-regulating the urokinase-type plasminogen activator system. Cancer Res 2003;63 (15):4648–55.
[33] Liu T, Bauskin AR, Zaunders J, Brown DA, Pankhurst S, Russell PJ, et al. Macrophage inhibitory cytokine 1 reduces cell adhesion and induces apoptosis in prostate cancer cells. Cancer Res 2003;63(16):5034–40.
[34] Kinsella TJ, Kunugi KA, Vielhuber KA, McCulloch W, Liu SH, Cheng YC. An in vivo comparison of oral 5-iodo-2′-deoxyuridine and 5-iodo-2-pyrimidinone-′-deoxyribose toxicity, pharmacokinetics, and DNA incorporation in athymic mouse tissues and the human colon cancer xenograft, HCT-116. Cancer Res 1994;54(10):2695–700.
[35] Pan SS, Johnson R, Gonzalez H, Thohan V. Mechanism of transport and intracellular binding of porfiromycin in HCT 116 human colon carcinoma cells. Cancer Res 1989;49(18):5048–53.
[36] Baek SJ, Kim JS, Jackson FR, Eling TE, McEntee MF, Lee SH. Epicatechin gallate-induced expression of NAG-1 is associated with growth inhibition and apoptosis in colon cancer cells. Carcinogenesis 2004;25(12):2425–32.
[37] Baek SJ, Kim JS, Moore SM, Lee SH, Martinez J, Eling TE. Cyclooxygenase inhibitors induce the expression of the tumor suppressor gene EGR-1, which results in the up-regulation of NAG-1, an antitumorigenic protein. Mol Pharmacol 2005;67(2):356–64.
[38] Baek SJ, Kim JS, Nixon JB, DiAugustine RP, Eling TE. Expression of NAG-1, a transforming growth factor-beta superfamily member, by troglitazone requires the early growth response gene EGR-1. J Biol Chem 2004; 279(8): 6883–92.
[39] Hazzalin CA, Cano E, Cuenda A, Barratt MJ, Cohen P, Mahadevan LC. p38/RK is essential for stress-induced nuclear responses: JNK/SAPKs and c-Jun/ATF-2 phosphorylation are insufficient. Curr Biol 1996;6(8):1028–31.
[40] Thorpe CM, Smith WE, Hurley BP, Acheson DW. Shiga toxins induce, super-induce, and stabilize a variety of C-X-C chemokine mRNAs in intestinal epithelial cells, resulting in increased chemokine expression. Infect Immun 2001;69(10):6140–7.
[41] Agarwal MK, Hastak K, Jackson MW, Breit SN, Stark GR, Agarwal ML. Macrophage inhibitory cytokine 1 mediates a p53-dependent protective arrest in S phase in response to starvation for DNA precursors. Proc Natl Acad Sci USA 2006;103(44):16278–83.
[42] Li PX, Wong J, Ayed A, Ngo D, Brade AM, Arrowsmith C, et al. Placental transforming growth factor-beta is a downstream mediator of the growth arrest and apoptotic response of tumor cells to DNA damage and p53 overexpression. J Biol Chem 2000;275(26):20127–35.
[43] Baek SJ, Wilson LC, Eling TE. Resveratrol enhances the expression of non-steroidal anti-inflammatory drug-activated gene (NAG-1) by increasing the expression of p53. Carcinogenesis 2002;23(3):425–34.
[44] Lee SH, Kim JS, Yamaguchi K, Eling TE, Baek SJ. Indole-3-carbinol and 3,3′-diindolylmethane induce expression of NAG-1 in a p53-independent manner. Biochem Biophys Res Commun 2005;328(1):63–9.
[45] Alfano D, Franco P, Vocca I, Gambi N, Pisa V, Mancini A, et al. The urokinase plasminogen activator and its receptor: role in cell growth and apoptosis. Thromb Haemost 2005;93(2):205–11.
[46] Gondi CS, Kandhukuri N, Dinh DH, Gujrati M, Rao JS. Down-regulation of uPAR and uPA activates caspase-mediated apoptosis and inhibits the PI3K/AKT pathway. Int J Oncol 2007;31(1):19–27.
[47] Cao DJ, Guo YL, Colman RW. Urokinase-type plasminogen activator receptor is involved in mediating the apoptotic effect of cleaved high molecular weight kininogen in human endothelial cells. Circ Res 2004;94(9):1227–34.
[48] Tkachuk N, Kiyan J, Tkachuk S, Kiyan R, Shushakova N, Haller H, et al. Urokinase induces survival or pro-apoptotic signals in human mesangial cells depending on the apoptotic stimulus. Biochem J 2008;415(2):265–73.
[49] Zhang X, Chaudhry A, Chintala SK. Inhibition of plasminogen activation protects against ganglion cell loss in a mouse model of retinal damage. Mol Vis 2003;9:238–48.
[50] Liang G, Wolfgang CD, Chen BP, Chen TH, Hai T. ATF3 gene. Genomic organization, promoter, and regulation. J Biol Chem 1996;271(3):1695–701.
[51] Hai T, Wolfgang CD, Marsee DK, Allen AE, Sivaprasad U. ATF3 and stress responses. Gene Expr 1999;7(4–6):321–35.
[52] Lu D, Wolfgang CD, Hai T. Activating transcription factor 3, a stress-inducible gene, suppresses Ras-stimulated tumorigenesis. J Biol Chem 2006; 281(15): 10473–81.
[53] Yamaguchi K, Lee SH, Kim JS, Wimalasena J, Kitajima S, Baek SJ. Activating transcription factor 3 and early growth response 1 are the novel targets of LY294002 in a phosphatidylinositol 3-kinase-independent pathway. Cancer Res 2006;66(4):2376–84.
[54] Yin X, Dewille JW, Hai T. A potential dichotomous role of ATF3, an adaptive-response gene, in cancer development. Oncogene 2007.
[55] Bottone Jr FG, Moon Y, Alston-Mills B, Eling TE. Transcriptional regulation of activating transcription factor 3 involves the early growth response-1 gene. J Pharmacol Exp Ther 2005;315(2):668–77.
[56] Nobori K, Ito H, Tamamori-Adachi M, Adachi S, Ono Y, Kawauchi J, et al. ATF3 inhibits doxorubicin-induced apoptosis in cardiac myocytes: a novel cardioprotective role of ATF3. J Mol Cell Cardiol 2002;34(10):1387–97.
[57] Selander KS, Brown DA, Sequeiros GB, Hunter M, Desmond R, Parpala T, et al. Serum macrophage inhibitory cytokine-1 concentrations correlate with the presence of prostate cancer bone metastases. Cancer Epidemiol Biomarkers Prev 2007;16(3):532–7.
[58] Chung YJ, Zhou HR, Pestka JJ. Transcriptional and posttranscriptional roles for p38 mitogen-activated protein kinase in upregulation of TNF-alpha expression by deoxynivalenol (vomitoxin). Toxicol Appl Pharmacol 2003;193(2):188–201.
[59] Harrison LM, van Haaften WC, Tesh VL. Regulation of proinflammatory cytokine expression by Shiga toxin 1 and/or lipopolysaccharides in the human monocytic cell line THP-1. Infect Immun 2004;72(5):2618–27.
[60] Moon Y, Uzarski R, Pestka JJ. Relationship of trichothecene structure to COX-2 induction in the macrophage: selective action of type B (8-keto) trichothecenes. J Toxicol Environ Health A 2003;66(20):1967–83.
[61] Martinez JM, Sali T, Okazaki R, Anna C, Hollingshead M, Hose C, et al. Drug-induced expression of nonsteroidal anti-inflammatory drug-activated gene/macrophage inhibitory cytokine-1/prostate-derived factor, a putative tumor suppressor, inhibits tumor growth. J Pharmacol Exp Ther 2006;318(2):899–906.
[62] Newman D, Sakaue M, Koo JS, Kim KS, Baek SJ, Eling T, et al. Differential regulation of nonsteroidal anti-inflammatory drug-activated gene in normal human tracheobronchial epithelial and lung carcinoma cells by retinoids. Mol Pharmacol 2003;63(3):557–64.
[63] Yamaguchi K, Lee SH, Eling TE, Baek SJ. A novel peroxisome proliferator-activated receptor gamma ligand, MCC-555, induces apoptosis via posttranscriptional regulation of NAG-1 in colorectal cancer cells. Mol Cancer Ther 2006;5(5):1352–61.
[64] Tran H, Maurer F, Nagamine Y. Stabilization of urokinase and urokinase receptor mRNAs by HuR is linked to its cytoplasmic accumulation induced by activated mitogen-activated protein kinase-activated protein kinase 2. Mol Cell Biol 2003;23(20):7177–88.
[65] Mazan-Mamczarz K, Lopez de Silanes I, Martindale JL, Atasoy U, Keene JD, Gorospe M. RNA-binding protein HuR enhances p53 translation in response to ultraviolet light irradiation. Proc Natl Acad Sci USA 2003;100(14): 8354–9.
[66] Wang W, Furneaux H, Cheng H, Caldwell MC, Hutter D, Liu Y, et al. HuR regulates p21 mRNA stabilization by UV light. Mol Cell Biol 2000; 20(3):760–9.
[67] Brooks SA, Connolly JE, Rigby WF. The role of mRNA turnover in the regulation of tristetraprolin expression: evidence for an extracellular signal-regulated kinase-specific, AU-rich element-dependent, autoregulatory pathway. J Immunol 2004;172(12):7263–71.